ZNF674: A New Krüppel-Associated Box–Containing Zinc-Finger Gene Involved in Nonsyndromic X-Linked Mental Retardation

Dorien Lugtenberg,[1] Helger G. Yntema,[1] Martijn J. G. Banning,[1] Astrid R. Oudakker,[1] Helen V. Firth,[3] Lionel Willatt,[3] Martine Raynaud,[4] Tjitske Kleefstra,[1] Jean-Pierre Fryns,[5] Hans-Hilger Ropers,[6] Jamel Chelly,[7] Claude Moraine,[4] Jozef Gécz,[8] Jeroen van Reeuwijk,[1,2] Sander B. Nabuurs,[2] Bert B. A. de Vries,[1] Ben C. J. Hamel,[1] Arjan P. M. de Brouwer,[1] and Hans van Bokhoven[1]

[1]Department of Human Genetics, Radboud University Nijmegen Medical Centre, and [2]Centre for Molecular and Biomolecular Informatics, Radboud University Nijmegen, Nijmegen, The Netherlands; [3]Department of Clinical Genetics, Addenbrooke's Hospital, Cambridge, United Kingdom; [4]Service de Génétique et INSERM U316, Hôpital Bretonneau, Tours, France; [5]Center for Human Genetics, University of Leuven, Leuven, Belgium; [6]Max Planck Institute for Molecular Genetics, Berlin; [7]INSERM 129-ICGM, Faculté de Médecine Cochin, Paris; [8]Department of Genetic Medicine, Women's and Children's Hospital and Department of Paediatrics, University of Adelaide, Adelaide

Array-based comparative genomic hybridization has proven to be successful in the identification of genetic defects in disorders involving mental retardation. Here, we studied a patient with learning disabilities, retinal dystrophy, and short stature. The family history was suggestive of an X-linked contiguous gene syndrome. Hybridization of full-coverage X-chromosomal bacterial artificial chromosome arrays revealed a deletion of ~1 Mb in Xp11.3, which harbors *RP2*, *SLC9A7*, *CHST7*, and two hypothetical zinc-finger genes, *ZNF673* and *ZNF674*. These genes were analyzed in 28 families with nonsyndromic X-linked mental retardation (XLMR) that show linkage to Xp11.3; the analysis revealed a nonsense mutation, p.E118X, in the coding sequence of *ZNF674* in one family. This mutation is predicted to result in a truncated protein containing the Krüppel-associated box domains but lacking the zinc-finger domains, which are crucial for DNA binding. We characterized the complete *ZNF674* gene structure and subsequently tested an additional 306 patients with XLMR for mutations by direct sequencing. Two amino acid substitutions, p.T343M and p.P412L, were identified that were not found in unaffected individuals. The proline at position 412 is conserved between species and is predicted by molecular modeling to reduce the DNA-binding properties of ZNF674. The p.T343M transition is probably a polymorphism, because the homologous *ZNF674* gene in chimpanzee has a methionine at that position. *ZNF674* belongs to a cluster of seven highly related zinc-finger genes in Xp11, two of which (*ZNF41* and *ZNF81*) were implicated previously in XLMR. Identification of *ZNF674* as the third XLMR gene in this cluster may indicate a common role for these zinc-finger genes that is crucial to human cognitive functioning.

Mental retardation (MR) is a complex and highly heterogeneous disorder with a prevalence of ~2% in the general population (American Association on Mental Retardation 2002). An estimated 13%–15% of MR is caused by mutations on the X chromosome (Mandel and Chelly 2004; Ropers and Hamel 2005). X-linked MR (XLMR) can be divided into syndromic and nonsyndromic forms. In the latter, MR is the only clinical feature observed. A total of 58 XLMR genes have been identified to date (Ropers and Hamel 2005): 37 genes for syndromic XLMR, 13 genes for nonsyndromic XLMR, and 8 genes that are causative for both syndromic and nonsyndromic XLMR.

The nonsyndromic XLMR genes can be clustered into several groups on the basis of their function. One group consists of regulators and effectors of Rho guanine triphosphatases. A second group comprises genes involved in transcription regulation and chromatin remodeling. The third group is a mixture of genes that are in some way linked to RNA splicing, protein translation, or degradation or have a role in energy metabolism. The group of transcription regulators includes two zinc-finger genes, *ZNF41* (MIM 314995) and *ZNF81* (MIM 314998), that are involved in nonsyndromic XLMR. These zinc-finger genes encode members of one of the largest families of potential transcription regulators in the human genome, the Krüppel-type zinc-finger protein family. It has been estimated that up to 700 genes encode Krüppel-type Cys-2 His-2 (C2H2) zinc fingers, and one-third of these also contain a Krüppel-associated box (KRAB) domain (Bellefroid et al. 1991). These KRAB-containing zinc-finger proteins (KRAB-ZFPs) are primarily regulators of transcription. There can be 3–20 zinc fingers in a zinc-finger protein, and each zinc finger recognizes a specific tri-

Received September 6, 2005; accepted for publication November 17, 2005; electronically published December 29, 2005.

Address for correspondence and reprints: Dr. Arjan P. M. de Brouwer, Department of Human Genetics, University Medical Centre St. Radboud, P.O. Box 9101, 6500 HB Nijmegen, The Netherlands. E-mail: A.debrouwer@antrg.umcn.nl

Am. J. Hum. Genet. 2006;78:265–278. 0002-9297/2006/7802-0009$15.00

Figure 1 The index patient with the deletion on Xp11.3, at age 5 years and 9 mo. There were no specific dysmorphic features observed.

nucleotide sequence in the promoter regions of target genes. The KRAB domain interacts with the KRAB-associated protein 1 (KAP-1) (Friedman et al. 1996). KAP-1 can interact with the heterochromatin protein HP1 and mediate gene-specific silencing (Ryan et al. 1999; Underhill et al. 2000). Most KRAB-ZFP genes are clustered at a number of regions in the genome. On the X chromosome, there is a KRAB-ZFP gene cluster at the Xp11 region (Knight et al. 1994), which includes *ZNF41* (Shoichet et al. 2003) and *ZNF81* (Kleefstra et al. 2004).

For the identification of approximately two-thirds of the known XLMR genes, positional cloning strategies have proven to be successful. These strategies include linkage analysis, the analysis of fragile sites, and the analysis of cytogenetic aberrations such as inversions, deletions, duplications, and translocations. For studying these chromosomal aberrations, array-based comparative genomic hybridization (array CGH) is a new powerful technique (Carter and Vetrie 2004). In a single hybridization experiment, small deletions and duplications can be detected throughout the genome. Mapping of deletions by using array CGH to identify the disease-causing gene has already been successful for CHARGE syndrome (MIM 214800) (Vissers et al. 2004). Recently, we published the development and validation of a full-coverage X-chromosomal BAC array (Veltman et al. 2004). In that study, the sensitivity and specificity of this high-resolution tiling clone set was shown for the detection of deletions and duplications as small as 100 kb on the X chromosome. Here, we have used the X-chromosomal BAC array to screen for aberrations in a child with learning disabilities, retinal dystrophy, and short stature. The family history was suggestive of an X-linked disorder. Array CGH exposed a deletion of ~1 Mb on Xp11.3, which harbors several candidate genes for XLMR. Two predicted Krüppel-type zinc-finger genes from the deleted region, *ZNF673* and *ZNF674*, were characterized. Sequence analysis of patients with nonsyndromic XLMR revealed that *ZNF674* is a new gene for nonsyndromic XLMR.

Material and Methods

Propositus

A boy aged 5 years and 9 mo was seen in the genetics clinic (fig. 1). He was the third son of healthy, unrelated parents and had two healthy brothers and a healthy sister. He was born at term weighing 2,730 g (9th percentile). Early developmental milestones were normal; he sat at 6 mo and walked at 13 mo. At age 8 mo, a squint was noted, and he was found to be myopic. His speech development was rather slow, and he did not talk in phrases until nearly age 2 years. In early childhood, he was investigated for failure to thrive, and he developed intolerance to dairy products. He was noted to have low IgG and IgA levels and was prescribed prophylactic antibiotics for 1 year. His immunoglobulin levels subsequently normalized. He was attending a school for children with moderate learning disability. On examination, he was a short child (height 0.99 m, <0.4th percentile) with microcephaly (occipital-frontal circum-

ference 46 cm, <0.4th percentile). He had a high, narrow palate and micrognathia. Ophthalmological review identified mild pigmentary changes in the periphery of both eyes, and electroretinogram findings were suggestive of a rod/cone retinal dystrophy. A cranial CT scan was reported to show no structural anomalies. At age 9 years, bilateral papilloedema was noted on ophthalmological review, and, after full investigation, he was given the diagnosis of benign intracranial hypertension and commenced treatment with acetazolomide. He currently attends a special school for children with visual impairment. Both healthy brothers have normal development, vision, and height (99.6th percentile), and the healthy sister also has normal development, vision, and height (75th–91th percentile). The father of the propositus has a height of 1.78 m (50th–75th percentile), and the mother has a height of 1.63 m (25th–50th percentile). The affected maternal cousin has a similar phenotype as the propositus, with short stature, low weight (<0.4th percentile), severe myopia (−10.5 D), and developmental delay. His mother has normal vision, normal development, and a height of 1.65 m (50th–75th percentile).

Families with XLMR and Controls

For array CGH, genomic DNA from the index patient was isolated using standard procedures and was purified using a QIAamp kit (Qiagen) in accordance with the instructions of the manufacturer. For mutation analysis, DNA from 337 mentally retarded males collected by the European XLMR consortium was available for sequencing. This group includes 28 families with linkage to the Xp11.3 region: 11 families with a positive LOD score >2 and 17 families with a positive LOD score <2. The additional 309 index patients were from families with a family history suggestive of X-linked inheritance. Previously, the index patient of each family was karyotyped, and mutations in the *FMR1* gene and in most known nonsyndromic XLMR genes located in the linkage interval were excluded. In addition, a total of 380 white control X chromosomes were available (from 190 males and 95 females). All samples were obtained after informed consent was obtained.

Array Preparation, Labeling, and Hybridization

The genomic X-chromosomal BAC array slides were prepared and validated as described elsewhere (Veltman et al. 2004). Labeling and hybridization were performed essentially as described elsewhere (Veltman et al. 2002). In brief, genomic DNA was labeled by random priming with Cy3-dUTP or Cy5-dUTP (Amersham Biosciences). Test and reference samples were mixed with 120 μg Cot-1 DNA (Roche) and then were coprecipitated and resuspended in 120 μl of a hybridization solution containing 50% formamide, 10% dextran sulfate, 2 × saline sodium citrate (SSC), 4% SDS, and 10 μg/μl yeast tRNA (Invitrogen). After denaturation of probe and target DNA, hybridization and posthybridization washing procedures were performed using a GeneTac Hybridization Station (Genomic Solutions) in accordance with the manufacturer's instructions. In brief, an 18-h hybridization with active circulation of the probe was performed, followed by five posthybridization wash cycles in 50% formamide and 2 × SSC at 45°C and five wash cycles in phosphate-buffered saline at 20°C. Slides were dried by centrifugation after a brief wash in water.

Image Analysis and Processing

Slides were scanned and imaged on an Affymetrix 428 scanner using the Affymetrix 428 scanner software package (version 1.0). The acquired microarray images were analyzed using Genepix Pro 5.0 (Axon Instruments) as described elsewhere (Veltman et al. 2002). For all calculations, we used the median of the pixel intensities minus the median local background for each dye per spot. Data normalization was performed per array subgrid by applying Loess curve fitting with a smoothing factor of 0.1 to predict the $\log_2$ transformed test-over-reference (T/R) value on the basis of the average logarithmic fluorescent intensities. Clones with an SD >0.3 were excluded, as were clones with <2 replicates remaining after this analysis.

PCR Analysis of Deletion in Xp11.3

To verify the deletion detected by array CGH, PCR was performed using primer sets amplifying the STS markers *DXS1146* and *STSG45963* outside the deleted region and proximal to *UTX* (5′-GGGTAATGTCAGTCCTCTTGC-3′ and 5′-CCAGCAATGAACAAGTGGAAG-3′) and distal to *RP2* (5′-ATACCCCATGCCCAGTTTC-3′ and 5′-CCACAAGGTCAAGACAAGTCAG-3′). Multiplex PCR was performed in a PTC-200 Peltier Thermal Controller (Biozym), with cycling conditions of 35 cycles at 95°C for 30 s, 60°C for 30 s, and 72°C for 45 s and 1.5 mM $MgCl_2$.

5′ and 3′ RACE

Rapid amplification of cDNA ends (RACE) was performed as described in the manufacturer's protocol (Clontech SMART RACE). In brief, a 5′ RACE PCR product was obtained by amplifying human fetal brain Marathon-Ready cDNA (Clontech) with adapter primer 1 (AP1) and a *ZNF674*-specific primer (5′-GAAAGTTTAAATGTGTTTTGAACACC-3′) designed for exon 6. For the 3′ end, adapter primer 2 (AP2) and a *ZNF674*-specific primer (5′-GTGCAGTGAACATGGGAAAGCCTCTG-3′) were used. For the nested PCR, nested AP1 (NAP1) and NAP2 were used in combination with a specific *ZNF674* primer (5′-ACCTGAAGATCACATCTGGCTTCC-3′ and 5′-GGAAAGCCTTTGGGGAGAAGTCAACC-3′, respectively). The following thermal cycle profiles were used for both the first PCR and the nested PCR: 1 min at 94°C; 5 cycles for 30 s at 94°C and 4 min at 72°C; 5 cycles for 30 s at 94°C and 4 min at 70°C; and 20 cycles for 20 s at 94°C and 4 min at 68°C. PCR products were sequenced, and 5′ and 3′ ends were identified.

RNA Isolation and Expression Studies

Epstein-Barr virus–immortalized human B-lymphocyte cell lines (EBV-LCLs) were grown to a density of 0.7×10^6 cells per ml of RPMI 1640 medium (Gibco) containing 10% fetal calf serum (Sigma), 1% penicillin-streptomycin (Gibco), and 1% GlutaMAX (Gibco). A total of 25×10^6 cells were harvested by centrifugation at 200 *g* for 5 min at room temperature and were resuspended in 500 μl of 8 mM Na_2HPO_4, 2 mM KH_2PO_4, 137 mM NaCl, and 2.7 mM KCl (pH 7.2). RNA was isolated using RNA-Bee (Tel-Test) and was further purified using the RNaesy Mini Kit (Qiagen) in accordance with the manufacturer's protocol. Total RNA was treated with

DNase I while bound to the RNaesy column, to remove residual traces of genomic DNA. Copy DNA was synthesized from 4 μg of total RNA by M-MLV reverse transcriptase (Invitrogen), in accordance with the manufacturer's protocol, with the use of random primers.

Mutation Analysis

PCR products covering the entire coding sequence of all genes in the deleted regions were amplified using genomic DNA from 28 families with nonsyndromic XLMR with a linkage interval on the X chromosome. For the *ZNF674* gene, an additional 309 patients with XLMR were screened for coding exons 3–6. Exon 6 was amplified in four overlapping fragments (6a, 6b, 6c, and 6d; see table 1). After purification with a Qiagen PCR purification kit, PCR products were directly sequenced on an Applied Biosystem 3730 automated sequencer by using the same primers used in the PCR.

Segregation and Control Analysis

For detection of mutation c.352G→T, a primary fragment was generated using the primers for fragment 6a (table 1), followed by *Fok*I (New England Biolabs) digestion (resulting in wild-type fragments of 188, 169, and 132 bp and in mutant fragments of 357 and 132 bp). For detection of mutation c.1028C→T, PCR amplification was followed by *Hpy*CH4IV (New England Biolabs) digestion. For both digestions, fragments were analyzed on a 1.5% agarose gel.

ARMS Analysis

Screening of the c.1235C→A mutation in exon 6 in 350 unrelated control individuals was performed by amplification-refractory mutation system (ARMS) analysis. We designed ARMS primers for both the wild-type and the mutant allele, with wild-type forward primer 5′-AGAGAATTCATACAGGAGAGAAATC-3′ and mutant forward primer 5′-AGAGAATTCATACAGGAGAGAAATA-3′. For a reverse primer, 5′-ATCAGTGGTGACTTCTCACTAAAGG-3′ was used. Amplification was performed with an annealing temperature of 60°C for the mutant allele and 56°C for the wild-type allele and with an $MgCl_2$ concentration of 1.5 mM.

Molecular Modeling

The effect of the P412L mutation on the DNA-binding capacity of ZNF674 was investigated using the crystal structure of a designed zinc-finger protein bound to DNA (PDB entry 1MEY [Kim and Berg 1996; see RCSB Protein Data Bank Web site]). A model was constructed for amino acid residues 385–463 of ZNF674, comprising three zinc-finger domains and their connecting linkers. The sequence identity between target and template for this region was 59%. The amino acid side chains in the model were positioned by SCWRL3.0 (Canutescu et al. 2003). Subsequently, the model was refined using YASARA, which was shown to increase model accuracy (Krieger et al. 2004). The quality of the final models was evaluated using WHAT CHECK (Hooft et al. 1996), which compares structural features of the model with a database of high-resolution x-ray structures. This resulted in quality scores comparable to those of medium-resolution crystal structures. Coordinate files are available on request.

Sequence Analysis and Phylogeny of Human ZNF674 Homologues

Approximately 500 human homologues of ZNF674 were identified by homology searches with full-length protein sequence of ZNF674 by performing three iterations of PSI-BLAST (Altschul et al. 1997; BLAST Web site) with the human subset in a nonredundant protein database (National Center for Biotechnology Information [NCBI], July 2005). Protein sequences were aligned by MUSCLE (Edgar 2004) by using the neighbor-joining method as implemented in Clustal (Saitou and Nei 1987), and a distance matrix was created for phylogenetic analysis. A subset of 32 protein sequences from a branch containing ZNF674 was used for realignment by MUSCLE and subsequent construction of a phylogenetic tree by PHYML (Guindon and Gascuel 2003).

Results

Array CGH Analysis

X-chromosomal BAC arrays (Veltman et al. 2004) were used to screen a family with possible X-chromosomal aberrations for deletions and duplications. The family

Table 1

Primers and PCR Conditions for Direct Sequencing of *ZNF674* Coding Sequences

	Primer Sequence (5′→3′)	
Exon	Forward	Reverse
3	ATTCTTCCCAGGGTGCAAAG	CCAGAAGAGGGGATAATTGG
4	GCTGAAGGTGGCACGGCCTC	TAGGGTGGCGGCGAAGACTG
5	AAGCTTCCAGAAAGGACAGG	ATCACCGAGGCCGTGCCACC
6a	GCTTGGGCATTTAGGGATTAG	CTCCCCAGTTTGACTTCTCTG
6b	CCCTAATCAACGAGGGAAAG	TGTTCACTGCACTGAGGTTTC
6c	GGTATTAAATGTACTACGTCCA	GCATTCATAGGGTCTCTCTCC
6d	GAATGCAGAAGATGTGGGAAAG	CAAATAATGAGACTAGTAATAGTC

Note.—For all PCRs, the annealing temperature was 60°C and the $MgCl_2$ concentration was 1.5 mM.

consisted of an affected boy and his maternal cousin with a similar clinical presentation, characterized by short stature, learning disabilities, and visual impairment due to retinal dystrophy. The pattern of inheritance and phenotype strongly suggested a contiguous gene-deletion syndrome on the X chromosome. Array CGH revealed a deletion of ~1 Mb located on Xp11.3 (fig. 2*A*). The deleted region encompasses 12 BAC clones, of which RP11-281E23 and RP11-101C24 have an intermediate $\log_2$ ratio and were thus suspected to span the breakpoints. The presence, size, and location of this deletion were confirmed by FISH analysis (data not shown). The deletion was delineated by PCR analysis of STS markers inside and outside the deleted region. This analysis confirmed that the deletion end points were located in BAC clones RP11-281E23 and RP11-101C24, and the dele-

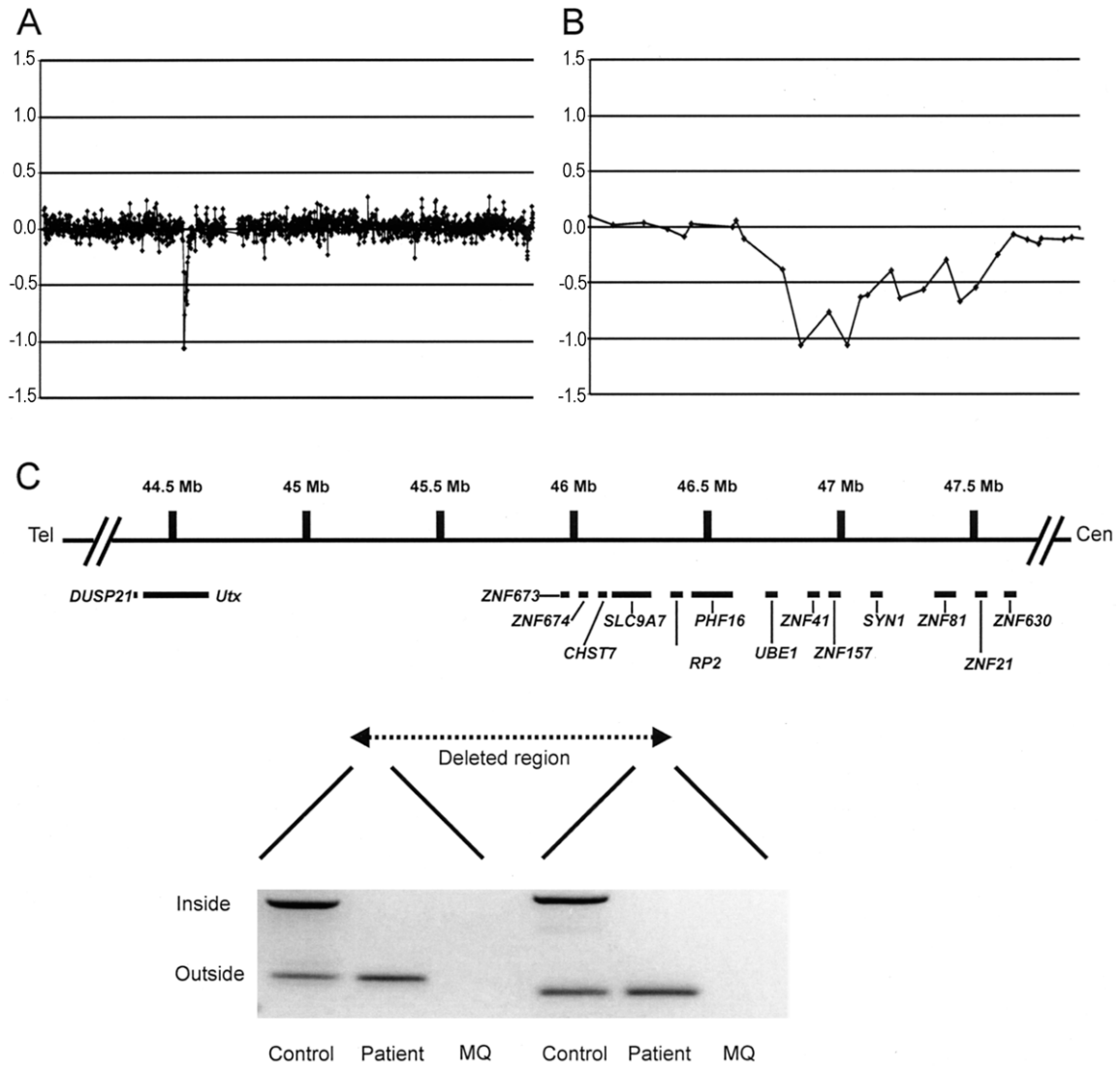

Figure 2 Array CGH profiles of the deletion in the index patient. *A*, X-chromosome array CGH profile of the index patient with a deletion in Xp11.3 of ~1 Mb. *B*, Enlarged, detailed view of the 1-Mb deletion in Xp11.3. The *X*-axis displays the Mb position of the clones on the X chromosome, ordered from Xpter to Xqter on the basis of genomic position (see full-genome BAC rearrays at Genome Sciences Center Web site). Each dot represents the mean $\log_2$ transformed and less-normalized test-over-reference (T/R) intensity ratio for each clone (*Y*-axis). Clones are represented by six independent replica spots on the array. *C*, Schematic overview of the part of Xp11 that includes the deleted region and the zinc-finger gene cluster (UCSC Human Genome Browser). The deleted region is indicated (*horizontal arrow*), and all deleted genes are shown. For the zinc-finger gene cluster, all genes are shown, and a number of the neighboring genes are also depicted. The deletion was confirmed and fine mapped by duplex PCR analysis with primer sets inside and outside the deleted region. Cen = centromere; Tel = telomere; MQ = Milli Q.

tion was shown to be 1.2 Mb. At the proximal side, the breakpoint is located between exons 3 and 4 of *RP2* (MIM 312600), and, at the distal side, the breakpoint is located between *ZNF673* and *UTX* (MIM 300128). Furthermore, FISH analysis revealed that this deletion segregated with the phenotype in this family, and X-inactivation studies showed that both carrier females had a complete skewed X-inactivation pattern (data not shown).

Selection of XLMR Candidate Genes

The affected boy carries a deletion affecting three known genes, *RP2, SLC9A7* (MIM 300368), and *CHST7* (MIM 300375), and two hypothetical zinc-finger genes, *ZNF673* and *ZNF674* (fig. 2*C*). The retinal dystrophy is likely to be a result of disruption of the *RP2* gene, one of the genes associated with X-linked retinitis pigmentosa (MIM 312600) (Schwahn et al. 1998). The other genes might play a role in the learning disability and short stature. The solute carrier family 9 isoform 7 (SLC9A7) is a sodium-hydrogen exchanger, which regulates ion transport. The carbohydrate sulfotransferase 7 (CHST7) belongs to the sulfotransferase family. Sulfotransferases generate sulfated glycosaminoglycan moieties during chondroitin sulfate biosynthesis. Both *SLC9A7* and *CHST7* genes are widely expressed, with only moderate expression in brain. Because the zinc-finger genes *ZNF41* (Shoichet et al. 2003) and *ZNF81* (Kleefstra et al. 2004) have been implicated in nonspecific XLMR, *ZNF673* and *ZNF674* were the prime candidate genes for the mental disability. *ZNF673* and *ZNF674* are highly similar both at the cDNA level (66.4% identity) and in their amino acid sequence (80.7% identity) until the first stop codon in *ZNF673* (fig. 3*A*). The predicted gene sequences of *ZNF673* and *ZNF674* were confirmed by PCR on a Marathon fetal-brain cDNA bank, with use of specific primers inside the predicted exons. Full-length sequences were determined by 5′ and 3′ RACE. The hypothetical ZNF673 protein appeared to encode KRAB A and B domains but no zinc-finger domains, because of the numerous stop codons in exon 6 of all mRNAs analyzed (fig. 3*B*). These stop codons are partially caused by an insertion of an adenine at position c.452, but additional stop codons are present in all reading frames. The *ZNF674* cDNA encodes a protein with KRAB A and B domains and 11 Krüppel-type C2H2 zinc-finger domains (fig. 3*C*). The transcript of *ZNF674* (GenBank accession number AY971607; Human Genome Organisation) has an ORF of 1,743 bp (582 aa), with a methionine start codon at position c.212 and a TGA stop codon at position c.1955 (fig. 3*B*). The start codon fulfills the Kozak criterion (A/GNNATGG) with the AAGATGG sequence. *ZNF674* is expressed in fetal brain, EBV-LCLs, and testis, as shown by PCR of cDNA (data not shown).

Sequence Analysis

Probands from 28 families with nonsyndromic XLMR with linkage to Xp11.3 were screened for mutations in the *SLC9A7, CHST7, ZNF673,* and *ZNF674* genes. Analysis of *ZNF674* revealed nonsense mutation c.352G→T (p.E118X) in family T040 in exon 6 that fully segregates with the phenotype (fig. 4*A*). All carrier females showed skewed X-inactivation patterns, whereas noncarriers of the mutation had normal random X-inactivation patterns (Raynaud et al. 2000). Previously, the MR in this family was linked to the *ZNF674* region, with a positive LOD score of 1.5 for markers *MAOA, AR,* and *DXS424* (Raynaud et al. 2000). Recently, recalculation of the LOD score with three additional family members (III-4, IV-1, and IV-2 in fig. 4*A*) resulted in a positive LOD score of 2.51 for the *AR* marker and a reduced linkage interval, containing *ZNF674*, with flanking markers *MAOA* and *DXS1217*. X-chromosomal aberrations >100 kb had been excluded earlier in this family by array CGH analysis (Lugtenberg et al. 2005). RT-PCR analysis revealed that the p.E118X mutation is also present in the mRNA, indicating that this mutation does not lead to complete reduction of mutant mRNA. This is expected because the mutation resides in the last exon, which means that the aberrant transcript is probably not prone to nonsense-mediated decay (Carter et al. 1996). The altered amino acid lies in the region between the KRAB domain and the zinc-finger domains. Hence, a truncated protein is predicted to lack the 462 C-terminal amino acids, including all zinc fingers. This mutation was not present in 349 control X chromosomes. Family T040 consists of six affected males (fig. 4*A*) presenting with moderate-to-severe nonsyndromic MR (table 2). The mother of the proband had normal intelligence. The proband was examined at age 17 years and had an intelligence quotient (IQ) of 45. He was the second son of unrelated parents and had one affected brother, three healthy sisters, and one carrier sister with borderline intelligence. In the *ZNF673* and *CHST7* genes, no nucleotide changes were identified. In the coding sequence of the *SLC9A7* gene, one silent change, c.1087G→A (p.A323A), was found in exon 6. These genes were not analyzed further, because of the absence of mutations in the families linked to Xp11.3.

The identification of a stop mutation in *ZNF674* compelled us to analyze other patients from families with XLMR. An additional 309 families with XLMR without a linkage interval were tested, revealing two additional nucleotide changes. In family D008, transversion c.1235C→A was found in exon 6 (fig. 4*B*). This variance causes the substitution of a leucine for a proline at position

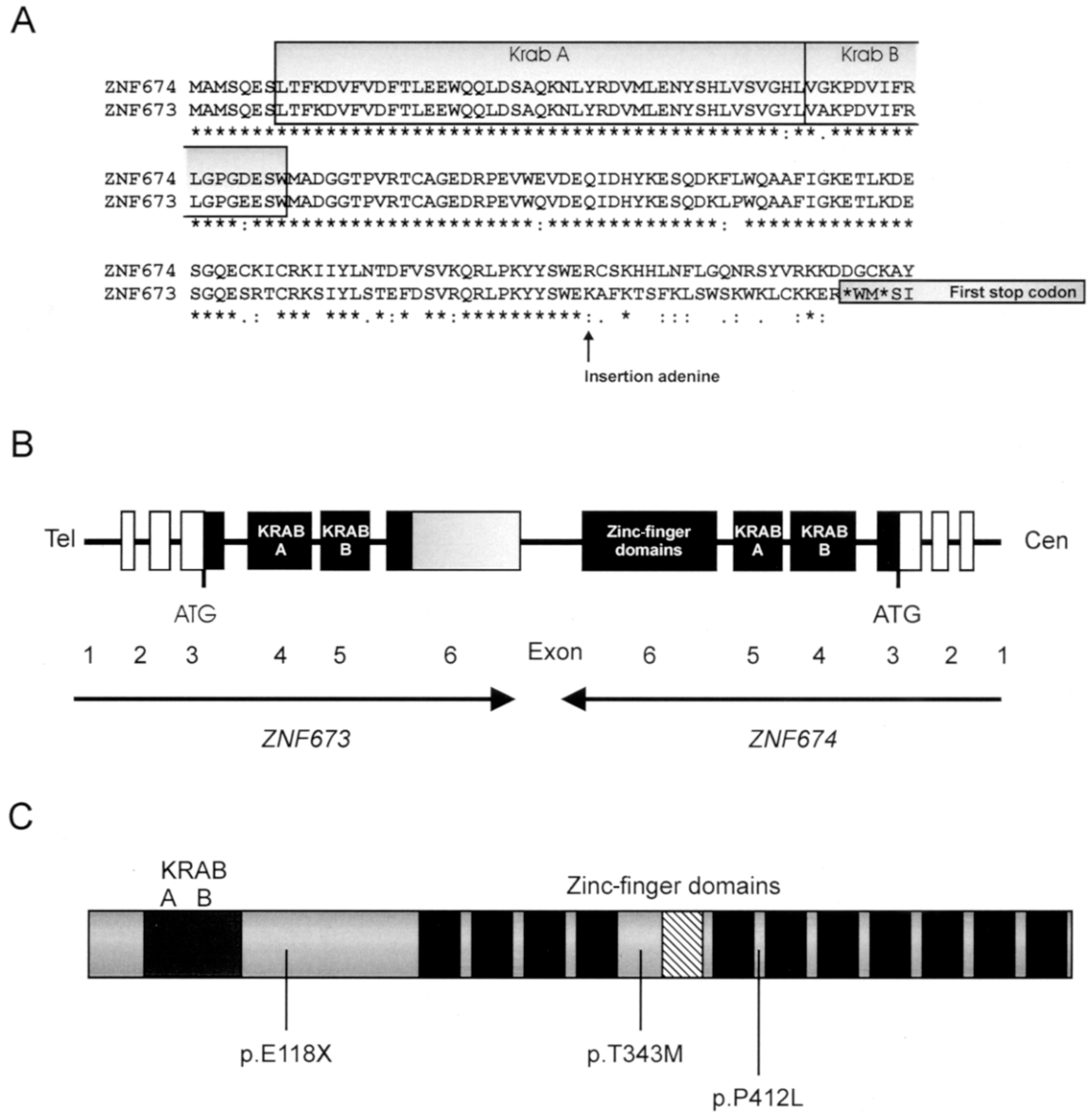

Figure 3 Compositions of *ZNF673* and *ZNF674* and their proteins. *A,* Alignment of ZNF673 and ZNF674 amino acid sequences, showing very high homology for the KRAB A and B domains. In ZNF673, an early stop codon results in a protein without zinc-finger domains. The vertical line indicates the insertion of one adenine at position c.452 in exon 6 of *ZNF673,* resulting in the premature stop codon at position c.514. *B,* Schematic picture of the gene structure of *ZNF673* and *ZNF674*. Coding sequence starts in exon 3. Exons 4 and 5 encode the KRAB A and B domains, respectively. In *ZNF674,* 11 zinc fingers are encoded by exon 6. Cen = centromere; Tel = telomere. *C,* The predicted ZNF674 protein. The positions of the amino acid changes are indicated. The 11 intact zinc-finger domains are represented by black boxes. The hatched box represents a degenerated pseudofinger that lacks one C residue, which is critical for the binding of a zinc atom.

412 and was not present in 362 control X chromosomes. Family D008 was previously described as carrying an inherited autosomal translocation, t(18;21)(q22.1q21.3). Both affected males had partial trisomy 21 and monosomy 18 and have severe MR, short stature, and other anomalies (Horn et al. 2003) (fig. 4*B*). The nucleotide change in *ZNF674* is present in both affected males and in the mother of the index patient. Another nucleotide change in exon 6, c.1028C→T, was identified in family P063. This transition predicts a substitution of a methionine for a threonine at position 343, which segregates with the phenotype (fig. 4*C*) and was not found in 354 control X chromosomes. This family consists of three affected males with moderate-to-severe MR. For two affected males, a clinical description is given in table 2. Pregnancy and delivery of these patients were uneventful.

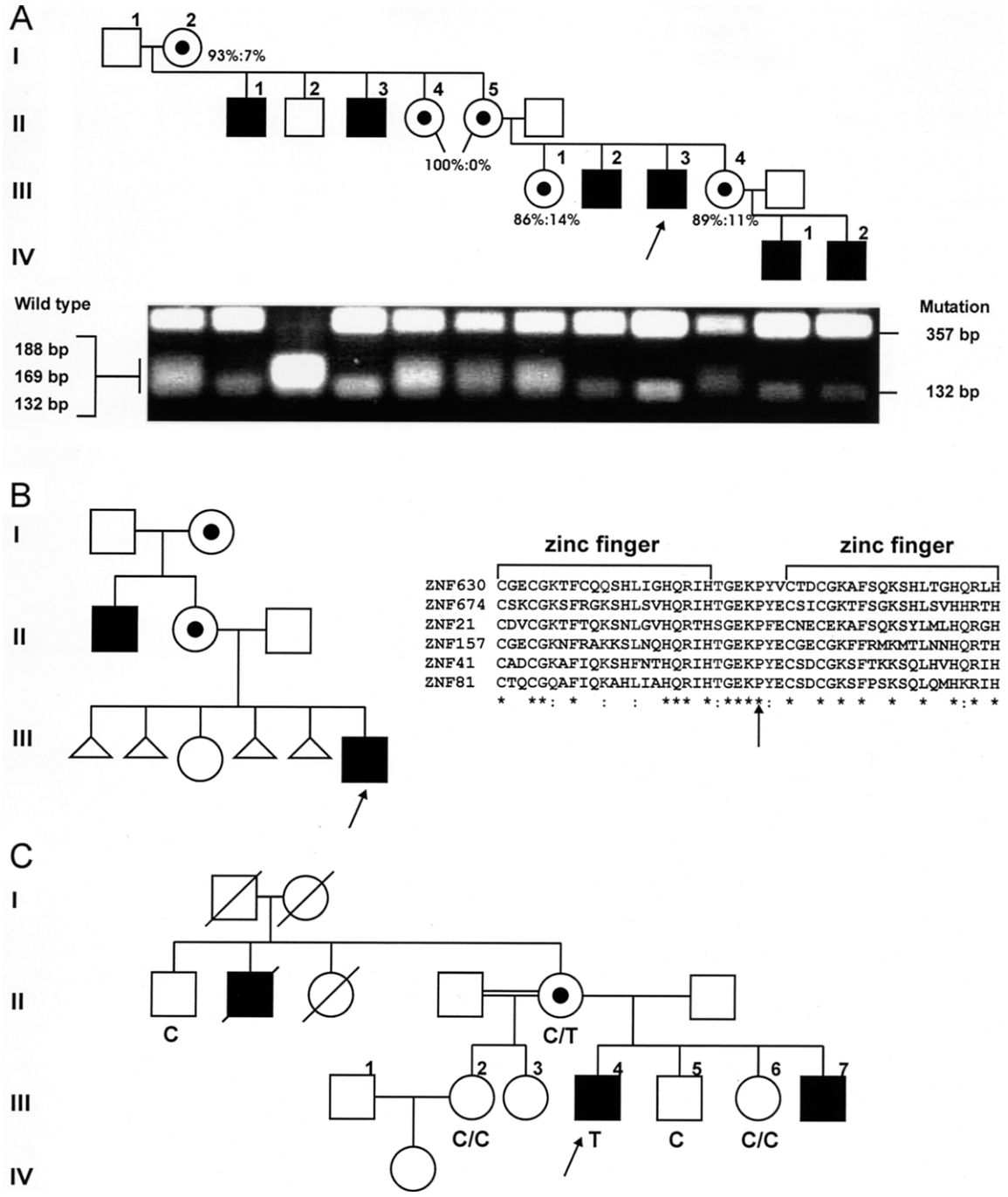

Figure 4 Segregation analyses of the three nucleotide changes. Segregation of all nucleotide changes in families T040 (*A*), D008 (*B*), and P063 (C) are shown. *A,* The c.352G→T mutation was tested in all family members available. The proband is indicated with an arrow. PCR products were digested using *Fok*I enzyme. From the wild-type DNA, three digestion products are formed that are 188, 169, and 132 bp in size. If the mutation is present, two products are formed that are 357 and 132 bp in size. *B,* For the segregation analysis of the c.1235C→A substitution, PCR products were sequenced for the proband (*arrow*), his mother, and an affected uncle. Conservation of the proline residue is indicated by a sequence alignment of all known zinc-finger genes in Xp11. *C,* In family P063, six family members were available for segregation analysis by direct sequencing, including the proband (*arrow*). Results are depicted for the tested family members.

Table 2

Clinical Characteristics of Individuals in Families T040 and P063

	Family T040						Family P063	
Characteristic	II-1	II-3	III-2	III-3	IV-1	IV-2	III-4	III-7
Birth weight, full term (g)	3,250	3,250	3,600	3,000	ND	1,750	2,520	3,050
Age at examination (years)	54	51	34	17	5	1.5	22	16
Height (SDs)	−3	−2.4	0	−1.2	ND	0	−1	<−2
Occipital-frontal circumference (cm)	57.2	56	58.2	57	ND	ND	54.4	54
Seizures	−	−	−	−	−	−	−	−
Facial dysmorphic features	Blepharophimosis	Blepharophimosis	−	−	−	−	Down-slanted ears, mild hypotelorism, deep palate	Down-slanted ears, atrophic tongue, deep palate
Other malformations	−	−	−	−	−	−	Small testes	Small testis
Other features	−	−	−	−	−	−	Myopic (−19 D/−23 D)	Myopic (−13 D/−16 D)
Age when first walking (mo)	18	12	18	18	ND	ND	30	ND
Age when continence acquired (mo)	24	24	72	36	ND	ND	ND	ND
MR severity	Moderate (IQ 40)	Severe (IQ 20)	Moderate (IQ 45)	Moderate (IQ 45)	Mild (IQ 64)	ND	Mild to severe	Severe
Education	Special school	Special school	Special school	Special school	−	−	Special school	Special school
Behavior	Obsessive	Autistic	−	−	−	−	−	−

Note.—ND = not determined; a minus sign (−) = not observed.

Patient III-4 has moderate-to-severe MR with good social skills and weak language abilities, mainly echolalic, with very poor syntax and phonological troubles. Patient III-7 has severe MR and requires special education.

Molecular Modeling of P412L

The P412L mutation is located in the linker region between the fifth and sixth zinc finger of ZNF674. The sequence of this linker is identical to the highly conserved TGEKP consensus sequence found in many zinc-finger proteins. Although it does not directly interact with the DNA itself, the linker region has been shown to be important for DNA binding (Foster et al. 1997; Laity et al. 2000). A model of the zinc-finger domains 5, 6, and 7 of ZNF674 was built using the known structure of another zinc-finger protein, 1MEY, as a template (fig. 5). This model was used to analyze the effects of the p.P412L mutation. Nuclear magnetic resonance studies indicate that the TGEKP linker between fingers is flexible in the protein but becomes more rigid upon binding the DNA (Foster et al. 1997; Wuttke et al. 1997). Proline rigidifies the connection between the linker and the first β-strand of the following finger; additionally, it stacks on the first highly conserved aromatic residue of the subsequent finger (Y413). Our model predicts that the P412L mutation disrupts the strong hydrophobic interaction with Y413. Furthermore, the conformational restriction that proline imposes is not preserved. Together, this raises the entropic cost of imposing ordered structure in the linker, and we therefore predict that the P412L mutation will weaken DNA binding of ZNF674. This prediction is supported by previous studies that have shown that substitution of the proline residue in the TGEKP sequence reduces the DNA binding of TFIIIA by a factor of 10 (Choo et al. 1993) and has a major deleterious effect on the DNA binding of ADR1 (Thukral et al. 1991).

Discussion

In this study, we identified a deletion on Xp11.3 in a patient with learning disability, retinal dystrophy, and short stature. The deletion contains five genes: *RP2, CHST7, SLC9A7, ZNF673,* and *ZNF674*. Disruption of the *RP2* gene is likely causative for the retinal dystrophy in this patient. Zinc-finger proteins have been implicated in XLMR; therefore, *ZNF673* and the novel *ZNF674* gene in this region were the prime candidates for the mental disability of this patient. Sequence analysis of additional patients from families with XLMR revealed three nucleotide changes in *ZNF674*: one nonsense mutation in a family with linkage to Xp11 and two amino acid changes in families without a linkage

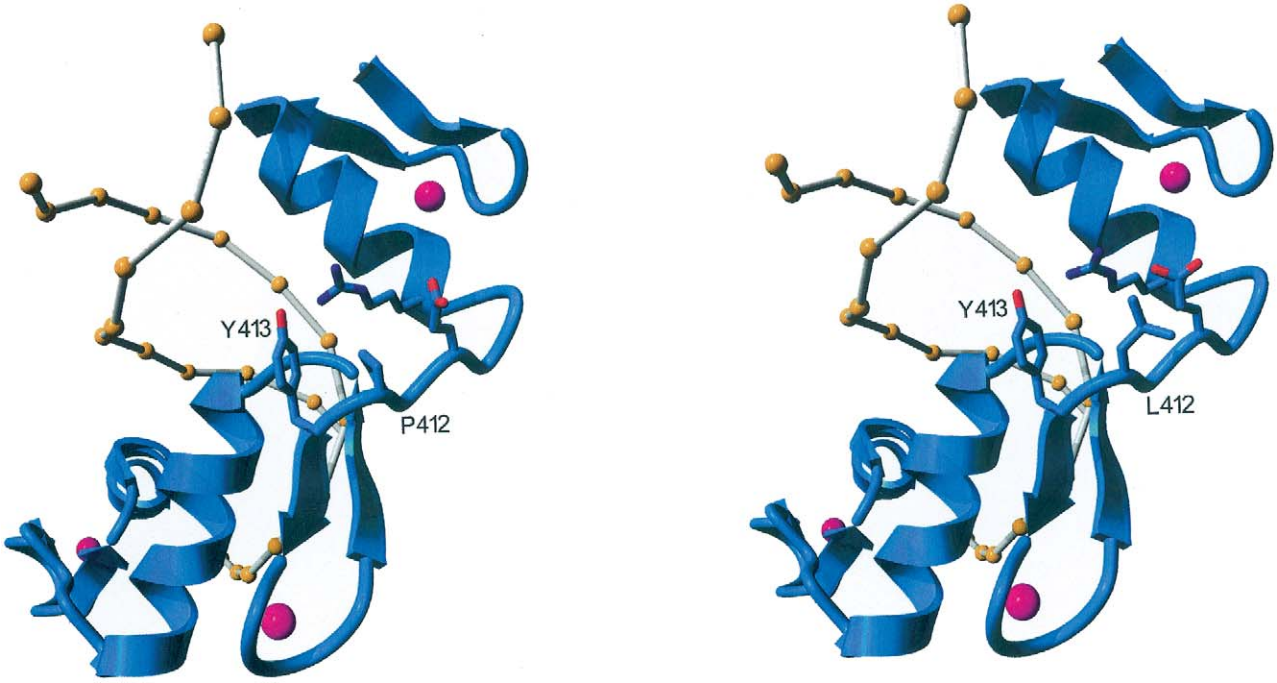

Figure 5 Molecular modeling of p.P412L mutation in family D008. The DNA double helix is depicted as balls and sticks. The three adjacent zinc-finger domains consist of two β-sheets (*arrows*) and one α-helix (*blue ribbon*) per domain. Pink balls represent zinc atoms that are bound to the zinc-finger domains. The position of the mutated proline amino acid in the linker sequence between two zinc-finger domains is colored red. This figure was made using YASARA (see YASARA Web site).

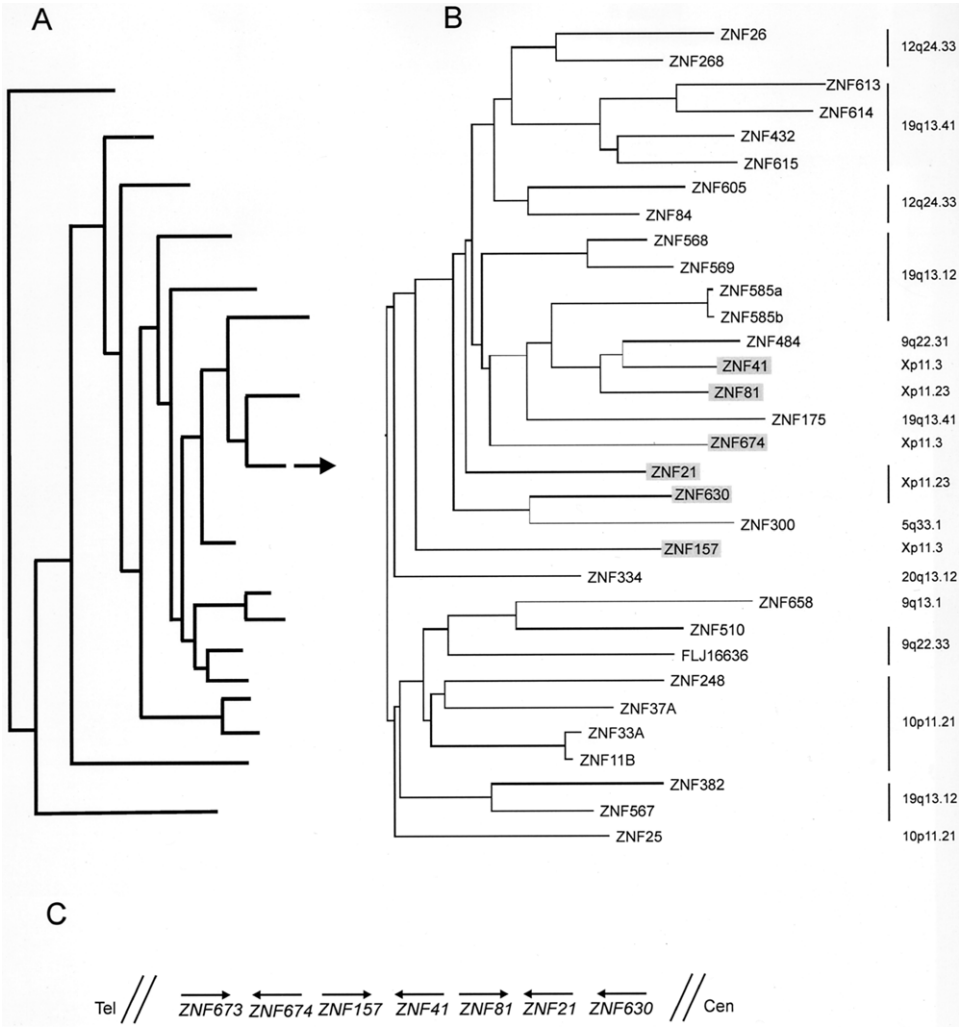

Figure 6 Sequence alignments of ZNF674 protein. *A,* Complete tree of the sequence alignments from the position-specific iterated BLAST of the protein sequence of ZNF674 versus all human proteins. *B,* Phylogenetic subtree of 32 protein sequences, including all zinc-finger genes from the Xp11 cluster (*gray boxes*). *C,* Schematic representation of the genomic organization of the zinc-finger gene cluster on Xp11. Three paired sets were identified with the same orientation and a single zinc-finger gene (*ZNF630*). Each set includes a nonsyndromic XLMR gene present (*ZNF41, ZNF81,* or *ZNF674*). Cen = centromere; Tel = telomere.

interval. Two other genes that are disrupted by the deletion, *CHST7* and *SLC9A7,* might contribute to other parts of the phenotype of the index patient, such as short stature. Mutation analysis in males with unexplained growth retardation should establish such a role.

The exact function of *ZNF674* is currently unknown, but other zinc-finger genes are reported to be involved in development and disease (Ladomery and Dellaire 2002). ZNF674 belongs to the Krüppel-type zinc-finger protein family, one of largest families of transcriptional regulators in the human genome. ZNF674 contains a KRAB domain and 11 C2H2 zinc-finger domains. The highly conserved KRAB domain binds to KAP-1 (Friedman et al. 1996), which subsequently recruits HP1 and other proteins to form a multiprotein nuclear receptor corepressor (N-CoR) complex (Underhill et al. 2000). This complex also includes histone-modifying proteins such as histone deacetylase 3 and SET domain, bifurcated 1 (SETDB1), which is a histone H3, lysine 9–specific methyltransferase (Schultz et al. 2002). This complex mediates the formation of a heterochromatin environment on a target promoter, which results in gene silencing. XLMR genes that are involved in transcription regulation and chromatin remodeling share similar domains with proteins in the KRAB-ZFP/KAP-1 repression complex. These observations suggest that mutations in these genes lead to MR via similar mechanisms. For instance, SETDB1 has a methyl CpG-binding domain that is related to the methyl CpG-binding protein MeCP2 (MIM 300005) (Ballestar and Wolffe 2001). KAP-1 needs

its plant homeodomain finger and bromodomain for effective gene silencing (Schultz et al. 2001). Plant homeodomain finger domains are also encoded by *ATRX* (MIM 301040) (Gibbons et al. 1995) and *JARID1C* (MIM 300534) (Jensen et al. 2005), which are both mutated in syndromic and nonsyndromic MR. Finally, the three zinc-finger genes *ZNF41, ZNF81,* and *ZNF674* all have a KRAB domain, which is important in gene silencing. The finding of a third zinc-finger gene that is involved in transcription regulation underlines the importance of this mechanism in neuronal development.

The p.E118X mutation in ZNF674 is predicted to result in a truncated protein with only KRAB A and B domains. This truncated protein lacks the 462 C-terminal aa and has a similar structure as that of the predicted ZNF673 protein, although 54 aa shorter. A function for a KRAB domain without zinc fingers has not been proposed. Obviously, this truncated protein is not capable of DNA binding because of the loss of the zinc fingers. It might still bind to its corepressor KAP-1 and interact with the N-CoR complex. In family D008, a missense mutation results in a substitution of a leucine for a highly conserved proline (fig. 4*C*). The proline is located in a linker between two zinc-finger domains and is important for the side-by-side orientation of the zinc-finger domains to efficiently bind DNA (fig. 5). In our models for ZNF674, P412 exhibits tight hydrophobic interactions with Y413. These interactions are lost when the proline at position 412 is substituted with a leucine. Also, substitution of the proline introduces additional conformational freedom in the linker, further imbalancing the structure for efficient and stable DNA binding. The affected males in family D008 also carry a partial monosomy 18 and trisomy 21 due to an unbalanced translocation, t(18;21)(q22.1;q21.3) (Horn et al. 2003). Therefore, we cannot conclude that the P412L mutation is causative for the severe MR of the two males. The T395M change found in family P063 does not involve one of the conserved domains. Moreover, in the predicted amino acid sequence of a putative orthologue of ZNF674 in chimpanzee, this threonine residue is replaced by a methionine. Therefore, it is unlikely that this is a disease-causing mutation, despite the fact that this sequence variance was not found in 354 control chromosomes. Functional analysis should give more insight into the effects of these sequence variants.

In Xp11, three zinc-finger genes have been described to be involved in XLMR—*ZNF41*, *ZNF81,* and *ZNF674*. These genes are part of a KRAB-ZFP gene cluster in this region, which includes *ZNF673, ZNF674, ZNF157* (MIM 300024) (Derry et al. 1995), *ZNF41* (Shoichet et al. 2003), *ZNF81* (Kleefstra et al. 2004), *ZNF21* (MIM 314993) (Knight et al. 1994), and *ZNF630*. A position-specific iterated BLAST with the full-length ZNF674 protein sequence versus all human proteins revealed a subtree of 32 proteins derived from a tree of 500 proteins total. Six Xp11 zinc-finger proteins were located in this subtree, confirming that they are highly similar to one another (fig. 6*A* and *B*). Since ZNF763 consists only of a KRAB domain, it was not present in the ZNF674 full-length protein subtree. Furthermore, the XLMR genes *ZNF41, ZNF81,* and *ZNF674* are located in the same branch. In contrast, *ZNF21, ZNF157,* and *ZNF630,* in which no mutation has been identified yet (authors' unpublished data), are positioned outside this branch. A similar analysis was done for the KRAB domain and the C2H2 zinc-finger domains of ZNF674, revealing comparable phylogenetic trees. All seven Xp11 zinc-finger genes were located in one branch of the tree. Phylogenetic analysis of the full-length ZNF674 protein revealed a potential mouse orthologue of ZNF21. Further analysis of the homologous region in mice showed an additional KRAB-ZFP gene that is probably the mouse orthologue of *ZNF157*. For the other human zinc-finger genes in this cluster, no mouse orthologues were found. It seems that the seven human KRAB-ZFP genes in Xp11 originate from duplication events involving the *ZNF21* and *ZNF157* genes. In chimpanzee, there seems to be seven zinc-finger genes in this cluster as well. These observations suggest that this KRAB-ZFP gene cluster is expanded independently in primate and rodent lineages after divergence. We speculate that these lineage-specific transcription factors have a significant impact on species-specific aspects of biology, such as neurogenesis.

Acknowledgments

We thank the families for their cooperation in this research. We are indebted to C. Beumer for culturing the patient cell lines. We also thank J. Bokhorst for expert technical assistance. This work was supported by grant QLG3-CT-2002-01810 (EURO-MRX) from the European Union and grant H02.10 (HGY) from the Hersenstichting Nederland.

Web Resources

The accession number and URLs for data presented herein are as follows:

BLAST, http://www.ncbi.nlm.nih.gov/BLAST/
GenBank, http://www.ncbi.nlm.nih.gov/Genbank/ (for transcript of *ZNF674* [accession number AY971607])
Genome Sciences Center, http://www.bcgsc.ca/lab/mapping/bacrearray/human/ (for full-genome BAC rearrays)
Human Genome Organisation, http://www.gene.ucl.ac.uk/hugo/
NCBI, http://www.ncbi.nlm.nih.gov/
Online Mendelian Inheritance in Man (OMIM), http://www.ncbi.nlm.nih.gov/Omim/ (for *ZNF41, ZNF81,* CHARGE syndrome, *RP2, UTX, SLC9A7, CHST7,* X-linked retinitis pigmentosa, MeCP2, *ATRX, JARID1C, ZNF157,* and *ZNF21*)
RCSB Protein Data Bank (PDB), http://www.rcsb.org/pdb/ (for PDB entry 1MEY)

UCSC Human Genome Browser, http://genome.ucsc.edu/
YASARA, http://www.yasara.org/

References

Altschul SF, Madden TL, Schaffer AA, Zhang J, Zhang Z, Miller W, Lipman DJ (1997) Gapped BLAST and PSI-BLAST: a new generation of protein database search programs. Nucleic Acids Res 25:3389–3402

American Association on Mental Retardation (2002) Mental retardation: definition, classification, and systems of supports. 10th ed. American Association on Mental Retardation, Washington, DC

Ballestar E, Wolffe AP (2001) Methyl-CpG-binding proteins: targeting specific gene repression. Eur J Biochem 268:1–6

Bellefroid EJ, Poncelet DA, Lecocq PJ, Revelant O, Martial JA (1991) The evolutionarily conserved Kruppel-associated box domain defines a subfamily of eukaryotic multifingered proteins. Proc Natl Acad Sci USA 88:3608–3612

Canutescu AA, Shelenkov AA, Dunbrack RL Jr (2003) A graph-theory algorithm for rapid protein side-chain prediction. Protein Sci 12: 2001–2014

Carter MS, Li S, Wilkinson MF (1996) A splicing-dependent regulatory mechanism that detects translation signals. EMBO J 15:5965–5975

Carter NP, Vetrie D (2004) Applications of genomic microarrays to explore human chromosome structure and function. Hum Mol Genet 13:R297–R302

Choo Y, Klug A (1993) A role in DNA binding for the linker sequences of the first three zinc fingers of TFIIIA. Nucleic Acids Res 21:3341–3346

Derry JM, Jess U, Francke U (1995) Cloning and characterization of a novel zinc finger gene in Xp11.2. Genomics 30:361–365

Edgar RC (2004) MUSCLE: a multiple sequence alignment method with reduced time and space complexity. BMC Bioinformatics 5:113

Foster MP, Wuttke DS, Radhakrishnan I, Case DA, Gottesfeld JM, Wright PE (1997) Domain packing and dynamics in the DNA complex of the N-terminal zinc fingers of TFIIIA. Nat Struct Biol 4: 605–608

Friedman JR, Fredericks WJ, Jensen DE, Speicher DW, Huang XP, Neilson EG, Rauscher FJ III (1996) KAP-1, a novel corepressor for the highly conserved KRAB repression domain. Genes Dev 10:2067–2078

Gibbons RJ, Picketts DJ, Villard L, Higgs DR (1995) Mutations in a putative global transcriptional regulator cause X-linked mental retardation with α-thalassemia (ATR-X syndrome). Cell 80:837–845

Guindon S, Gascuel O (2003) A simple, fast, and accurate algorithm to estimate large phylogenies by maximum likelihood. Syst Biol 52: 696–704

Hooft RW, Vriend G, Sander C, Abola EE (1996) Errors in protein structures. Nature 381:272

Horn D, Neitzel H, Tonnies H, Kalscheuer V, Kunze J, Hinkel GK, Bartsch O (2003) Familial MCA/MR syndrome due to inherited submicroscopic translocation t(18;21)(q22.1q21.3) with breakpoint at the Down syndrome critical region. Am J Med Genet A 117:236–244

Jensen LR, Amende M, Gurok U, Moser B, Gimmel V, Tzschach A, Janecke AR, Tariverdian G, Chelly J, Fryns JP, Van Esch H, Kleefstra T, Hamel B, Moraine C, Gécz J, Turner G, Reinhardt R, Kalscheuer VM, Ropers HH, Lenzner S (2005) Mutations in the *JARID1C* gene, which is involved in transcriptional regulation and chromatin remodeling, cause X-linked mental retardation. Am J Hum Genet 76: 227–236

Kim CA, Berg JM (1996) A 2.2 Å resolution crystal structure of a designed zinc finger protein bound to DNA. Nat Struct Biol 3:940–945

Kleefstra T, Yntema HG, Oudakker AR, Banning MJ, Kalscheuer VM, Chelly J, Moraine C, Ropers HH, Fryns JP, Janssen IM, Sistermans EA, Nillesen WN, de Vries LB, Hamel BC, van Bokhoven H (2004) *Zinc finger 81* (*ZNF81*) mutations associated with X-linked mental retardation. J Med Genet 41:394–399

Knight JC, Grimaldi G, Thiesen HJ, Bech-Hansen NT, Fletcher CD, Coleman MP (1994) Clustered organization of *Krüppel* zinc-finger genes at Xp11.23, flanking a translocation breakpoint at OATL1: a physical map with locus assignments for ZNF21, ZNF41, ZNF81, and ELK1. Genomics 21:180–187

Krieger E, Darden T, Nabuurs SB, Finkelstein A, Vriend G (2004) Making optimal use of empirical energy functions: force-field parameterization in crystal space. Proteins 57:678–683

Ladomery M, Dellaire G (2002) Multifunctional zinc finger proteins in development and disease. Ann Hum Genet 66:331–342

Laity JH, Dyson HJ, Wright PE (2000) DNA-induced alpha-helix capping in conserved linker sequences is a determinant of binding affinity in Cys(2)-His(2) zinc fingers. J Mol Biol 295:719–727

Lugtenberg D, de Brouwer AP, Kleefstra T, Oudakker AR, Frints SG, Schrander-Stumpel CT, Fryns JP, Jensen LR, Chelly J, Moraine C, Turner G, Veltman JA, Hamel BC, de Vries BB, van Bokhoven H, Yntema HG (2005) Chromosomal copy number changes in patients with non-syndromic X-linked mental retardation detected by array CGH. J Med Genet (http://jmg.bmjjournals.com/cgi/content/abstract/jmg.2005.036178v1) (electronically published September 16, 2005; accessed December 12, 2005)

Mandel JL, Chelly J (2004) Monogenic X-linked mental retardation: is it as frequent as currently estimated? The paradox of the ARX (Aristaless X) mutations. Eur J Hum Genet 12:689–693

Raynaud M, Moizard MP, Dessay B, Briault S, Toutain A, Gendrot C, Ronce N, Moraine C (2000) Systematic analysis of X-inactivation in 19 XLMR families: extremely skewed profiles in carriers in three families. Eur J Hum Genet 8:253–258

Ropers HH, Hamel BC (2005) X-linked mental retardation. Nat Rev Genet 6:46–57

Ryan RF, Schultz DC, Ayyanathan K, Singh PB, Friedman JR, Fredericks WJ, Rauscher FJ III (1999) KAP-1 corepressor protein interacts and colocalizes with heterochromatic and euchromatic HP1 proteins: a potential role for Krüppel-associated box-zinc finger proteins in heterochromatin-mediated gene silencing. Mol Cell Biol 19: 4366–4378

Saitou N, Nei M (1987) The neighbor-joining method: a new method for reconstructing phylogenetic trees. Mol Biol Evol 4:406–425

Schultz DC, Ayyanathan K, Negorev D, Maul GG, Rauscher FJ III (2002) SETDB1: a novel KAP-1-associated histone H3, lysine 9-specific methyltransferase that contributes to HP1-mediated silencing of euchromatic genes by KRAB zinc-finger proteins. Genes Dev 16:919–932

Schultz DC, Friedman JR, Rauscher FJ III (2001) Targeting histone deacetylase complexes via KRAB-zinc finger proteins: the PHD and bromodomains of KAP-1 form a cooperative unit that recruits a novel isoform of the Mi-2α subunit of NuRD. Genes Dev 15:428–443

Schwahn U, Lenzner S, Dong J, Feil S, Hinzmann B, van Duijnhoven G, Kirschner R, Hemberger M, Bergen AA, Rosenberg T, Pinckers AJ, Fundele R, Rosenthal A, Cremers FP, Ropers HH, Berger W (1998) Positional cloning of the gene for X-linked retinitis pigmentosa 2. Nat Genet 19:327–332

Shoichet SA, Hoffmann K, Menzel C, Trautmann U, Moser B, Hoeltzenbein M, Echenne B, Partington M, van Bokhoven H, Moraine C, Fryns JP, Chelly J, Rott HD, Ropers HH, Kalscheuer M (2003) Mutations in the *ZNF41* gene are associated with cognitive deficits: identification of a new candidate for X-linked mental retardation. Am J Hum Genet 73:1341–1354

Thukral SK, Morrison ML, Young ET (1991) Alanine scanning site-directed mutagenesis of the zinc fingers of transcription factor ADR1:

residues that contact DNA and that transactivate. Proc Natl Acad Sci USA 88:9188–9192 (erratum 90:7908)

Underhill C, Qutob MS, Yee SP, Torchia J (2000) A novel nuclear receptor corepressor complex, N-CoR, contains components of the mammalian SWI/SNF complex and the corepressor KAP-1. J Biol Chem 275:40463–40470

Veltman JA, Schoenmakers EF, Eussen BH, Janssen I, Merkx G, van Cleef B, van Ravenswaaij CM, Brunner HG, Smeets D, Geurts van Kessel A (2002) High-throughput analysis of subtelomeric chromosome rearrangements by use of array-based comparative genomic hybridization. Am J Hum Genet 70:1269–1276

Veltman JA, Yntema HG, Lugtenberg D, Arts H, Briault S, Huys EH, Osoegawa K, de Jong P, Brunner HG, Geurts van Kessel A, van Bokhoven H, Schoenmakers EF (2004) High resolution profiling of X chromosomal aberrations by array comparative genomic hybridisation. J Med Genet 41:425–432

Vissers LE, van Ravenswaaij CM, Admiraal R, Hurst JA, de Vries BB, Janssen IM, van der Vliet WA, Huys EH, de Jong PJ, Hamel BC, Schoenmakers EF, Brunner HG, Veltman JA, van Kessel AG (2004) Mutations in a new member of the chromodomain gene family cause CHARGE syndrome. Nat Genet 36:955–957

Wuttke DS, Foster MP, Case DA, Gottesfeld JM, Wright PE (1997) Solution structure of the first three zinc fingers of TFIIIA bound to the cognate DNA sequence: determinants of affinity and sequence specificity. J Mol Biol 273:183–206